CHALMERS

TITLE OF PROJECT

Thesis for the degree of Master of Science

ANDREAS BÜLLING

Department of Mathematical Sciences
CHALMERS UNIVERSITY OF TECHNOLOGY
Gothenburg, Sweden 2012
Master's Thesis 2012:1

Abstract

Lorem ipsum dolor sit amet, consectetur adipisicing elit, sed do eiusmod tempor incididunt ut labore et dolore magna aliqua. Ut enim ad minim veniam, quis nostrud exercitation ullamco laboris nisi ut aliquip ex ea commodo consequat. Duis aute irure dolor in reprehenderit in voluptate velit esse cillum dolore eu fugiat nulla pariatur. Excepteur sint occaecat cupidatat non proident, sunt in culpa qui officia deserunt mollit anim id est laborum.

Acknowledgements

Lorem ipsum dolor sit amet, consectetur adipisicing elit, sed do eiusmod tempor incididunt ut labore et dolore magna aliqua. Ut enim ad minim veniam, quis nostrud exercitation ullamco laboris nisi ut aliquip ex ea commodo consequat. Duis aute irure dolor in reprehenderit in voluptate velit esse cillum dolore eu fugiat nulla pariatur. Excepteur sint occaecat cupidatat non proident, sunt in culpa qui officia deserunt mollit anim id est laborum.

The Authors, Location 11/9/11

Contents

1

Introduction

Short intro for this section

1.1 Background

Historically - LBM and modelling of electrohydrodynamics. Development til today.

1.2 General problem description

Description of problem + what we want to achieve in this work.

1.3 Outline

How is this report structured?

2

Electrohydrodynamics in microchannels

In this chapter, the fundamental physics behind electrokinetic flow, important for later discussions, will be presented. Particularly, a modelling approach based on the coupling of Navier-Stokes, Nernst-Planck and Poission's equations is given.

2.1 Basic concepts of electrokinetic flow

Electrohydrodynamics involves the study of electric phenomena on fluid flow. How fluids carrying electrical charges (electrolytes) react upon external electrical fields or interact with charged objects are examples of problems that arise in this field.

2.1.1 Electrical double layers

As a charged object is brought into contact with an electrolyte it is, qualitatively, easily deduced that ions with a sign of charge opposite to that of the object will be attracted to the object and ions with the same sign of charge will be repelled. These two distinct categories of ions will from hereon be referred to as counter- and co-ions respectively. In this case, for a neutral electrolyte, a surplus of counter-ions will be present in the direct vicinity of the object and a surplus of co-ions will be present at some other location further from the object.

The area with a surplus of counter-ions in an electrolyte in contact with a charged object is often referred to as an electrical double layer. Two distinct regions will be formed in this area, thus the name double layer. The two layers are often referred to as the Stern layer (adsorbed ions) and the diffusive layer (mobile ions). The Stern layer is usually several orders of magnitude thinner than the diffusive layer and is therefore seldom considered when it comes to modelling [1].

2.1.2 Electroosmosis

As fluid carrying a net charge, e.g. in the diffusive layer of an EDL, is under influence of an electric field, the charged particles will move due to the electric forces. As the charge particles move, they will affect the surrounding liquid, causing it move as well. This liquid motion is often referred to as electroosmotic flow. [1]

2.2 Complete physical model

To model the fluid motion of a charged fluid under influences of electrostatic forces, a coupling between different models is considered.

The electric field and potential in the system are obtained from solving Poisson's equation for electrostatics (section 2.3) with a given charge density. This Charge density is obtained from the Nernst-Planck equation (section 2.4) by including effects on the charge distribution from the electric field previously mentioned, diffusion and advection. The advective charge flux is given from the velocity field in the fluid that is obtained by solving the Navier-Stokes equations (section 2.5). Forces due to present electric fields on net charged areas of the fluid also couples the NS equations to the NP equation. More about the force coupling is discussed in sections. 2.6 and 2.7. The coupling between the different equations are visualised in fig. 2.1.

2.3 The potential - Poisson's equation

To be able to model the flow dynamics of liquids in a channel with present EDLs, the potential and charge distribution in the channel must be determined. These quantities are mutually related through Poisson's equation for electrostatics:

$$\nabla^2 \psi = -\frac{\rho_e}{\epsilon_r \epsilon_0} \tag{2.1}$$

where ψ is the electrical potential, ρ_e the electrical charge density, ϵ_r is the relative permittivity and ϵ_0 the vacuum permittivity. Under certain assumptions, the charge density may be explicitly determined as a function of the potential distribution, one such result is the so called Poisson-Boltzmann equation, further discussed in section 2.4.2.

2.3.1 Boundary conditions

At the charged boundaries, most physical situations may be covered by either specifying the potential or the surface charge density. The former would be a boundary condition of Dirichlet type:

$$\psi(\mathbf{x}) = \zeta(\mathbf{x}) , \ \mathbf{x} \in \Gamma \tag{2.2}$$

and the latter a boundary condition of Neumann type:

3
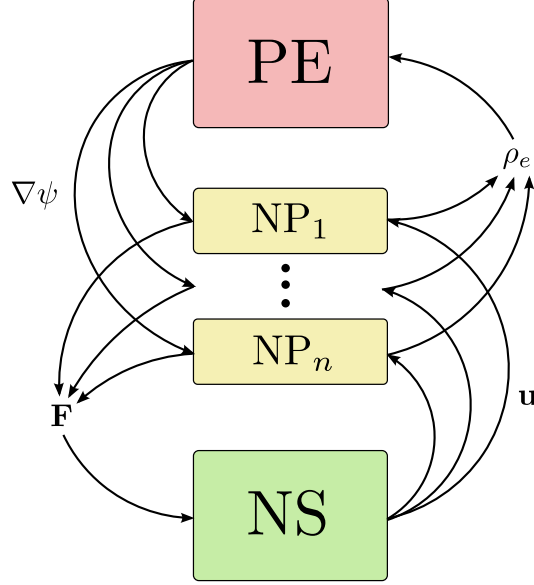
Figure 2.1: Visualisation of the coupling between the three equations present in the model. Poisson's equation (PE), The set of Nernst-Planck equations (NP_1 ... NP_n) and the Navier-Stokes equations (NS). The dependencies have also be marked with arrows indicating what quantities for a certain equation that are needed from an other.

$$\nabla \psi(\mathbf{x}) \cdot \mathbf{n} = -\frac{\sigma(\mathbf{x})}{\epsilon_0 \epsilon_r} \ , \ \mathbf{x} \in \Gamma \tag{2.3}$$

where Γ denotes the boundary of the domain and $\mathbf{n}$ is the normal to the boundary surface. [2]

2.4 The transport of charges - Nernst-Planck equation

The charge concentration in an electrolyte is indeed affected by its environment. In the model proposed here, influences from: advection of the electrolyte, diffusion due to concentration gradients and effects from the electric field originating from charged objects placed at the border or in the flow is considered. Charge conservation without any external sources of the ion density, $c(\mathbf{x}, t)$, gives:

$$\frac{\partial c}{\partial t} + \nabla \cdot \mathbf{J} = 0 \tag{2.4}$$

where $\mathbf{J}(\mathbf{x}, t)$ is the net flux induced by the effects described above. Explicit expressions for the fluxes due to advection and diffusion respectively are

$$\mathbf{J}_{adv} = c\mathbf{u} \tag{2.5}$$

and

$$\mathbf{J}_{dif} = -D\nabla c \tag{2.6}$$

where $\mathbf{u}$ is the advective velocity and D is a diffusion coefficient. The ionic flux due to the presence of an electric potential, $\psi(\mathbf{x}, t)$, is given by the Nernst equation [1]:

$$\mathbf{J}_{ele} = -\frac{zq_e D}{k_B T} c\nabla\psi \tag{2.7}$$

where z is the relative charge of an ion, q_e is the fundamental charge, k_B is the Boltzmann constant and T is the temperature of the fluid.

Summing up the fluxes and putting them into eq. (2.4) gives

$$\frac{\partial c}{\partial t} = \nabla \cdot \left[D\nabla c - c\mathbf{u} + \frac{zq_e D}{k_B T} c\nabla\psi \right] \tag{2.8}$$

which is a known result often referred to as the Nernst-Planck equation. The advective velocity, $\mathbf{u}$, and the potential gradient, $\nabla\psi$, are obtained from couplings to the Navier-Stokes and Poisson's equation respectively. More about the coupling between the equations is discussed in section 2.2.

2.4.1 Boundary conditions

Depending on the physical situation that is being modelled, different conditions may be imposed at the boundaries of the domain. Throughout this work, at hard boundaries (walls), the charge flux through the boundary is set to zero, i.e.:

$$\mathbf{J} \cdot \mathbf{n} = 0 \ , \ \mathbf{x} \in \Gamma \tag{2.9}$$

where $\mathbf{n}$ denotes the normal to the surface and Γ is the boundary of the domain.

2.4.2 Poisson-Boltzmann equation

Consider a system consisting of an electrolyte in contact with a (flat) charged wall. Under certain assumptions, it is possible to explicitly determine the charge density in eq. (2.8) as a function of the electric potential. E.g. if there is no advection present and if the system has reached a steady state, i.e. $\partial c/\partial t = 0$ and $\mathbf{u} = \mathbf{0}$ we have:

$$D\nabla c + \frac{zq_e D}{k_B T} c\nabla\psi = \alpha \tag{2.10}$$

where α is some arbitrary constant. Due to the steady state assumption, what the equation above actually says is that the net flux of charge in the system is constant. Since no flux of charge is wanted to flow through the wall boundary, the flux is set to zero on the wall and since the flux is constant it will therefore be zero everywhere in the liquid, i.e. $\alpha = 0$.

Considering only a one-dimensional situation with a position variable y varying in a direction out from the wall into the liquid, eq. (2.10) reads

$$\frac{1}{\text{c}}\frac{dc}{dy} + \frac{zq_e}{k_BT}\frac{d\psi}{dy} = 0. \tag{2.11}$$

The charge density is determined by solving eq. (2.11) for c, i.e. integrating the equation. In order to avoid introducing additional unknown quantities, the equation is integrated to far away from the wall where the potential from the EDL is assumed to have decreased to zero and where the concentrations, c^∞, of the electrolyte is known.

$$\int_y^\infty d\ln(\text{c}(y')) = -\frac{zq_e}{k_BT}\int_y^\infty d\psi(y') \tag{2.12}$$

This gives an expression for $C(y)$:

$$\text{c}(y) = \text{c}^\infty \exp\left(-\frac{zq_e\psi(y)}{k_BT}\right). \tag{2.13}$$

In a general case, there may be several species of ions in the electrolyte, the net charge density, ρ_e, is then given by simply summing up the contributions from the different species:

$$\rho_e = q_e \sum_i z_i\text{c}_i. \tag{2.14}$$

Summarising eqs. (2.1), (2.13) and (2.14) gives the Poisson-Boltzmann equation in one dimension

$$\frac{d^2\psi(y)}{dy^2} = -\frac{q_e}{\epsilon_r\epsilon_0}\sum_i z_i\text{c}_i^\infty \exp\left(-\frac{z_iq_e\psi(y)}{k_BT}\right). \tag{2.15}$$

The Debye–Hückel approximation

Historically, the non-linear nature of eq. (2.15) complicated when it came to solving it. This was a major difficulty in the past when the computational power at hands were rather limited. A linearisation is therefore sometimes done, this linear version of the PB equation is often referred to as the Debye–Hückel approximation. The solution of the linearisation gives, something to compare with and is usually used when defining a characteristic length scale of the EDL.

For a 1:1 electrolyte solution, eq. (2.15) reduces to

$$\frac{d^2\psi(x)}{dx^2} = \frac{2\text{c}^\infty q_e z}{\epsilon_r\epsilon_0}\sinh\left(\frac{zq_e\psi(x)}{k_BT}\right). \tag{2.16}$$

and the linearised equation is

$$\frac{d^2\psi(x)}{dx^2} = \frac{2\text{c}^\infty q_e^2 z^2}{\epsilon_r\epsilon_0 k_BT}\psi(x) = \kappa^2\psi(x) \tag{2.17}$$

where κ^{-1} is the Debye length and gives a measure for the characteristic size of the EDL.

Limitations of the Poisson-Boltzmann model

As the Poisson-Boltzmann equation is derived several assumptions are made. First, the net flux of ions are assumed to be zero and that the advective contribution the flux is negligible. Thus, the PB equation is only applicable when the system is at (or very close) thermodynamical equilibrium.

<p style="text-align:center;color:red;">TODO: Continue this discussion...</p>

2.5 The velocity field - Navier-Stokes equations

In hydrodynamics, the Navier-Stokes equations are one of the most fundamental corner stones. They describe the motion of a fluid under the influence of various internal and external forces.

For later convenience and for reference when it comes to deriving the Lattice-Boltzmann formulation of the NS equation, a brief sketch of a derivation will here be presented. A most general form of the Navier-Stokes equation follows from momentum conservation

$$\frac{\partial(\rho\mathbf{u})}{\partial t} + \nabla \cdot (\rho\mathbf{u} \otimes \mathbf{u}) + \mathbf{Q} = 0 \tag{2.18}$$

where, ρ is fluid density, $\mathbf{u}$ is velocity and $\mathbf{Q}$ is a momentum source term (force per volume). Expanding the time derivative and the divergence terms respectively gives

$$\mathbf{u}\left(\frac{\partial\rho}{\partial t} + \nabla \cdot (\rho\mathbf{u})\right) + \rho\left(\frac{\partial\mathbf{u}}{\partial t} + \mathbf{u} \cdot \nabla\mathbf{u}\right) + \mathbf{Q} = 0. \tag{2.19}$$

By assuring mass conservation (without sources) we have that

$$\frac{\partial\rho}{\partial t} + \nabla \cdot (\rho\mathbf{u}) = 0 \tag{2.20}$$

and eq. (2.19) reduces to

$$\rho\left(\frac{\partial\mathbf{u}}{\partial t} + \mathbf{u} \cdot \nabla\mathbf{u}\right) + \mathbf{Q} = 0 \tag{2.21}$$

which together with eq. (2.20) is a general formulation of the Navier stokes equations.

The force term $\mathbf{Q}$, is determined by the physical properties of the fluid and from its environment. In this work, only incompressible Newtonian fluids will be studied. The force contribution to $\mathbf{Q}$ involved in that case is limited to viscous forces, pressure gradients in the fluid and to external force fields. Putting that into eqs. (2.20) and (2.21) gives

$$\nabla \cdot \mathbf{u} = 0 \tag{2.22}$$

and

$$\rho \left(\frac{\partial \mathbf{u}}{\partial t} + \mathbf{u} \cdot \nabla \mathbf{u} \right) = -\nabla \mathrm{P} + \mu \nabla^2 \mathbf{u} + \mathbf{F} \tag{2.23}$$

where P is the pressure, μ the kinematic viscosity and $\mathbf{F}$ is the contributions from external forces.

2.5.1   Boundary conditions

At hard boundaries (walls), the boundary conditions to eqs. (2.22) and (2.23) are set on the velocity of either a Dirichlet or Neumann type. In most physical situations the Dirichlet condition is used which corresponds to that there is a friction between the fluid and the wall, usually full friction, i.e. when no relative movement between fluid and wall is present and the velocity at the wall boundary is set to zero, i.e.

$$\mathbf{u} = 0 \ , \ \ \mathbf{x} \in \Gamma \tag{2.24}$$

where Γ denotes the boundary. The Neumann type conditions are used for no-friction walls where the normal component of the derivative of the velocity is specified, usually to zero.

At wet boundaries, inlets and outlets, of the domain various boundary conditions may be set. For instance the pressure or the velocity could be fixed. In the case of a fixed pressure boundary, a flow direction must also be specified for completeness. [**?**]

2.6   Pressure-driven electrokinetic flow

As a charged fluid is driven by a pressure gradient, a movement of charges, i.e. an electrical current will be induced. Due to the charge flux, a potential gradient will build up along the flow direction. This potential is usually referred to as the streaming potential, $\phi(\mathbf{x})$, and its magnitude is determined from the induced current through Ohm's law

$$\mathbf{J} = -\sigma \nabla \phi \tag{2.25}$$

where σ is the conductivity of the fluid. For a perfectly conducting fluid, no potential difference will be built up. Also a complete neutral solution will carry no net current and therefore will no potential difference build up in that case either.

Charges under the influence of an electric field will be affected by a force. Charges moving due to this force will, in a liquid, also pull liquid (uncharged) molecules with them. In a macroscopic limit, the force density affecting the charges in the liquid is assumed to affect the liquid as whole. The volumetric force affecting the fluid from the presence of the streaming potential is then given by:
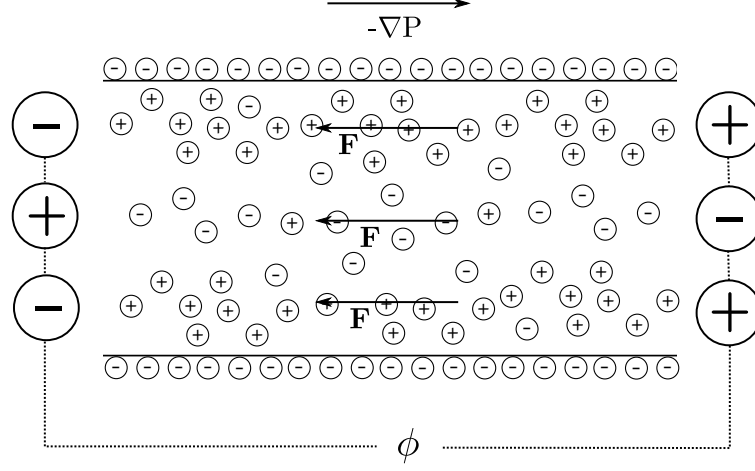
$$\mathbf{F} = -\rho_e \nabla \phi \tag{2.26}$$

Figure 2.2: Example of an electroviscous system. The fluid is driven by a pressure gradient, ∇P. The direction of the forces on the fluid. The force originates from the potential difference that builds up along the channel, ϕ. The force is always opposite to the flow direction, thus slowing the flow down.

where ρ_e is the charge density. This is an example of how the charge density from the Nernst-Planck equation may couple to the force term in Navier-Stokes equations.

This force will always be affecting the fluid in an direction opposite of that of the net flux of charge, i.e. the force will slow the fluid down, this is illustrated in fig. 2.2. This effect that a moving net charged fluid is slowed down is called the *electroviscous effect*. The name originates from that a similar effect might be achieved by increasing the viscosity of the fluid.

2.7 Electroosmotic flow

Instead of driving the fluid flow through a pressure drop, a net charged fluid may be driven by an external electric field. This may be seen as the opposite case to that in section 2.6 where a current is induced by a pressure drop.

The volumetric force on the fluid from the external field, $\mathbf{E}_{ext}$, is given by

$$\mathbf{F} = \rho_e \mathbf{E}_{ext} \tag{2.27}$$

where ρ_e is the charge density. If the electric field is constant (or at least has the same direction) everywhere, the sign of the force is not in the same direction for a net charged positive area of the fluid as for a net charged negative. Thus the fluid may be either slowed down or sped up. This is a qualitative difference to pressure driven situation and is illustrated in fig. 2.3.
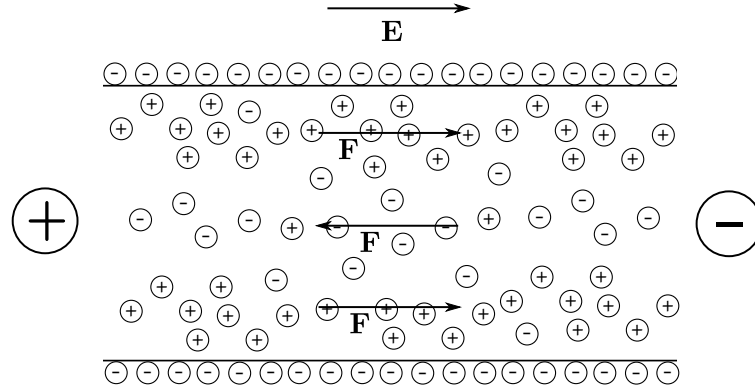
Figure 2.3: Example of an electroosmotic system. The fluid is driven by an external electric field, **E**. The direction of the forces on the fluid from the electric field is indicated with arrows. Note however that the fluid does not necessarily has to flow in the direction of the force, this due to viscous effects in the fluid.

The electroviscous effect is in the case of pure electroosmotic flow usually neglected as the field due to the streaming potential is, in most physical cases, small in comparison to the applied external field. [1]

3

The lattice-Boltzmann method

Rather than modelling on a macroscopic or microscopic scale, the lattice-Boltzmann method operates at a scale in between those, often referred to as a mesoscopic scale. Nowadays, the method is most frequently used in modelling fluid dynamics, i.e. solving the macroscopic Navier-Stokes equations. However, the lattice-Boltzmann method is not limited to this case and may be used to model other macroscopic systems as well. In this chapter a LBM approach will, in addition to the Navier-Stokes equations, also be formulated for the Nernst-Planck and the Poission's equation.

3.1 Historical overview

With the introduction of electronic calculating machines came also a completely new possibility of tackling problems. New fields of computational science was born and methods for solving both new and traditional problems were developed.

The idea of using a discrete and simplified version of the Boltzmann-equation dates back to the mid 60's [3] with an experimental attempt to model simple gas dynamics. However, at the time, this kind of statistical computational approaches was not considered a serious alternative for the modelling of more sophisticated and complex systems such as fluid behaviour. It was first in the mid 80's when Frisch, Hasslacher and Pomeau showed that a lattice automaton, with a lattice of certain symmetry and that conserved mass and momentum in the collisions, reproduced the Navier-Stokes equations in a macroscopic limit. It was by their work and the always increasing computational power that made the idea of fluid modelling on a mesoscopic scale a serious research topic. [4]

But the lattice gas automata (LGA) approach suffered from some flaws, e.g. that the boolean nature of the method introduced statistical noise and that lack of symmetry in the lattices used made the advection non-isotropic. The statistical noise was usually dealt with by averaging which resulted in a coarsed domain and the advection issue was

handled by introducing lattices of higher symmetry. As the flaws of the LGA approach was dealt with one after one, the method evolved into what we today know as the lattice-Boltzmann method, with the crucial refinement of using continuous distributions over boolean variables. [4]

Today, the lattice-Boltzmann method is in many situations indeed a competitor to more traditional CFD methods. For example with advantages when it comes to parallelisation or implementing boundary conditions in complex geometries. The downside with the LBM is the lack of theoretical work done and lack of literature compared to the case with traditional methods such as finite element/volume methods. [5]

3.2 Statistical background

Consider one litre of air. At NTP, the volume will contain in the order of 10^{22} molecules. In order to model this system microscopically, 6 variables per molecule will be needed to describe the microstate of the system. Just to store the state of the system in a computer would require more space than the estimated size of the whole world wide web times one million [6]. Thus, for these kind of systems, the microscopic approach is somewhat impractical.

Fortunately, statistical approaches have been developed for these kind of problems. A fundamental quantity used for describing the system is a continuous probability density distribution, f. This distribution function may be regarded as an average over the microstates. Consider a volume of $d^3\mathbf{x}d^3\mathbf{p}$ in phase space, the number of molecules, dN in this volume is then given through the density distribution, f as

$$dN(\mathbf{x}, \mathbf{p}, t) = f(\mathbf{x}, \mathbf{p}, t)d^3\mathbf{x}d^3\mathbf{p}. \tag{3.1}$$

Thus $f(\mathbf{x}, \mathbf{p}, t)$ is a measure for the number of particles at location $\mathbf{x}$ with momentum $\mathbf{p}$ at time t.

In the late 19th century, Boltzmann developed a model for the time evolution of f. To do this he had to make several assumptions. First, only collisions between two particles are considered, this makes the equation mostly applicable to dilute gases. Second, the two particles colliding are assumed to be uncorrelated before the collision. Third, external forces are assumed not to affect the collisions [4]. The equation is named after its father to the Boltzmann (transport) equation and reads:

$$\partial_t f + \frac{\mathbf{p}}{m} \cdot \nabla_{\mathbf{x}} f + \frac{\mathbf{F}}{m} \cdot \nabla_{\mathbf{v}} f = Q(f, f) \tag{3.2}$$

where f is the distribution function for a single species collection of particles of mass m, $\mathbf{F}$ is external forces, $\mathbf{p}$ is momentum, $\nabla_{\mathbf{x}}$ and $\nabla_{\mathbf{v}}$ are the gradients in location and velocity space respectively. The right-hand side contains the so called collision term which in the general case is expressed as an integral.

$$Q(f, f) = \int \int \tag{3.3}$$

This integral states how the distribution function changes after a two. However, the structure of this integral is in most physical situations too complicated to be used directly. Therefore, a number of simplifications have been proposed during the years.

When designing these approximations, at least two main properties of the collision integral must be kept. [4]

1. The same quantities that is conserved under collisions in the collsion integral must also be conserved in the approximation.

2. Boltzmann's H-theorem must also be fulfilled for the approximated collision operator.

Without being to specific, the H-theorem states that the entropy computed from f is always increasing with time and that the maximum entropy is obtained for a so called Maxwellian distribution in in momentum/velocity space. Boltzmann used an other quantity denoted by H closely related to entropy, thus the name of the theorem. The Maxwellian distribution in two dimensions that f tends towards is given by

$$f^{(M)}(\mathbf{x}, \mathbf{v}, t) = n \left(\frac{m}{2\pi k_B T} \right) \exp \left(-\frac{m}{2k_B T}(\mathbf{v} - \mathbf{u})^2 \right) \tag{3.4}$$

where $\mathbf{u}$ is the mean velocity of the particles in the system and $n(\mathbf{x})$ is the number of particles at location $\mathbf{x}$. In section 3.4, one of the most widely used approximations of the collision integral will be presented.

3.3 Basic idea of the LBM

As previously noted, the lattice-Boltzmann is a mesoscopic method. This means that the modelling is neither done on a microscopic (molecular) level nor by direct solving the macroscopic equations involved. The aim, in the most situations with the lattice-Boltzmann method is indeed to solve some macroscopic equation but not direct. Instead a statistical model is used with various mesoscopic variables that, in some limit, reproduces the macroscopic variables. It is also possible to ensure that these variables (to some extent) fulfil a certain macroscopic equation by using a certain scheme.

Basically the lattice-Boltzmann method solves a discretised version of eq. (3.2) for the distribution functions from which the macroscopic quantities then are determined. Both the spatial positions and the velocity space is discretised allowing the distributions to "sit" only at certain positions and to stream to neighbouring locations only in certain directions. Usually in two dimensions the velocity space is discretised into 9 distinct velocities, more about the choice of lattice is discussed in section 3.5. In this case 9 distribution functions are needed per node which might correspond to one or two macroscopic variables but is indeed fewer than the number of variables needed for a microscopic approach.

The discretised Boltzmann equation is referred to as the lattice-Boltzmann equation and is one of the fundamental corner stones in the lattice-Boltzmann method, it reads:

$$f_i(\mathbf{x} + \mathbf{c}_i \delta_t, t + \delta_t) - f_i(\mathbf{x}, t) = \Omega_{ij}(\mathbf{x}, t) \tag{3.5}$$

where f_i denotes the distribution function for direction $\mathbf{c}_i$, δ_t is the time step and Ω_i is the (for now non-specified) collision operator. An implicit sum over the j index i assumed. Various forms of collision operators exist and will be further discussed in section 3.4.

3.3.1 Computational algorithm

In order to solve eq. (3.5) the distribution functions must be set to some initial value. The choice of initial value is in most cases crucial with respect to stability and accuracy of the method. More about the initialisation will be discussed in later sections of this chapter.

When a proper initialisation has been performed, the time evolution of the distribution functions is determined iteratively by the explicit scheme in the LBE, eq. (3.5). The update in each time step is usually divided into two computational tasks. First is the new value that later will be propagated to a neighbouring node computed, i.e.

$$f_i(\mathbf{x}, t + \delta_t) = f_i(\mathbf{x}, t) + \Omega_{ij}(\mathbf{x}, t) \tag{3.6}$$

This step will be referred to as the collision step since it is here the "collision" is computed. The second step consists of propagating the distribution functions to the neighbouring node in its corresponding direction, i.e.

$$f_i(\mathbf{x} + \mathbf{c}_i \delta_t, t + \delta_t) = f_i(\mathbf{x}, t + \delta_t) \tag{3.7}$$

This step will be referred to as the streaming step.

In the case of a finite domain, certain rules (boundary conditions) must be specified at the boundaries. Typically the distribution functions that are going to be streamed out of the domain is used to define the unknown ones that will "enter" the domain. More about boundary conditions in section 3.11. Thus, at each time step, the boundary conditions must also be handled.

This is broadly the whole computational algorithm behind the LBM, in fig. 3.1 is a flow scheme of the algorithm is shown.

3.4 The BGK collision operator

The collision term in the LBE is the main ingredient in what determines the physics of the system that is beeing modelled. Here the desired interaction of the pseudo particles is stated. In section 3.2, two necessary properties to approximations of the full collsion integral was stated.

One of the simplest collision operators that fullfil conditions (1) and (2) in section 3.2 is the BGK operator (BGK from its creators: Bhatnagar, Gross and Krook). It was proposed in 1954 and is today one of the most comonly used collision operators both in the case of the Lattice-Boltzmann and the continuous Boltzmann equation. It is based
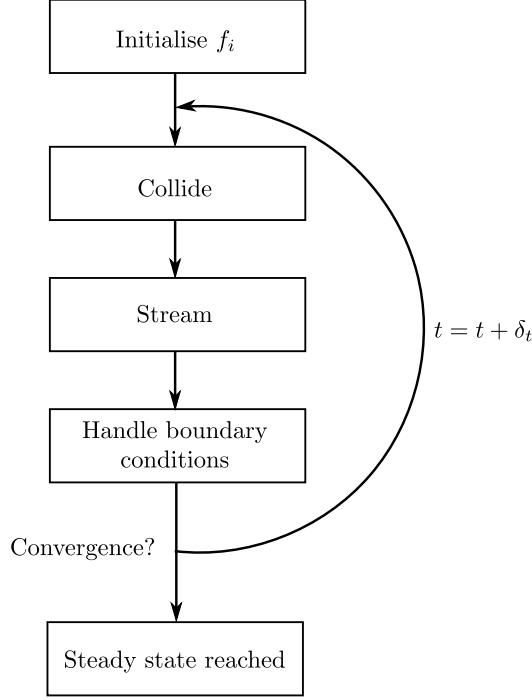
Figure 3.1: Flowchart of the most fundamental parts in an implementation of the LBM. The convergence is usually tested for a macroscopic variable.

on the principle of relaxing f towards a Maxwellian distribution. The relaxation is also performed in such a way that the collision invariants are preserved. In the discrete case, eq. (3.5) the operator is given by:

$$\Omega_{ij} = \Omega_i = -\omega \left[f_i(\mathbf{x}, t) - f_i^{(eq)}(\mathbf{x}, t) \right] \tag{3.8}$$

where ω is a parameter determining the relaxation rate and $f_i^{(eq)}$ should be an equilibrium distribution that makes sure that f satisfies the nescessary conditions. In the discrete case, a truncated expansion of eq. (3.4) is typically used [4]. This gives

$$f_i^{(eq)} = w_i \rho \left[1 + \frac{\mathbf{c}_i \cdot \mathbf{u}}{c_s^2} + \frac{(\mathbf{c}_i \cdot \mathbf{u})^2}{2c_s^4} - \frac{\mathbf{u}^2}{2c_s^2} \right] \tag{3.9}$$

where ρ is the zeroth moment of f_i and $\mathbf{c}_i$ is a unit velocity in the discretised velocity space.

The BGK operator is due to its simplicity both when it comes to theoretical treatment and implementation a popular choice. However in some physical situations, e.g. multiphase or high Reynolds-number flows, more sophisticated alternatives are required [4]. Throughout this work, the BGK operator will be used.
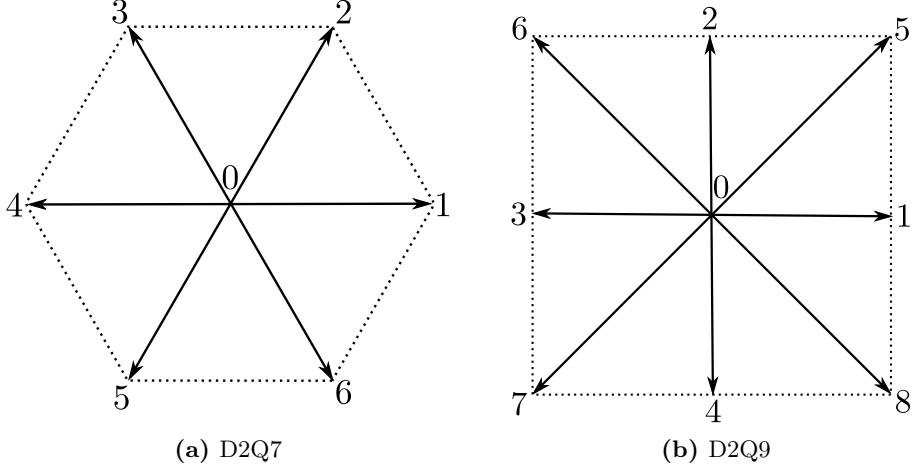
15

(a) D2Q7   **(b)** D2Q9

Figure 3.2: Two different unit cells for lattices used in the LBM in two dimensions. In (a) the D2Q7 seven speed lattice is shown and in (b) the nine speed D2Q9 lattice. The numbering at the edges is the usual naming convention for the different velocities.

3.5   The lattice

The discrete spatial coordinates together with the discrete velocity coordinates forms a lattice. Spatial coordinates are neighborwise connect through the discrete velocities. The discretisation in the LBM must be performed in such a way that the lattice may be produced from translating a single unit cell. This gives that the spatial resolution is constant for the whole domain. In other approaches, e.g. finite element methods the mesh may locally be refined at interesting regions of the domain which is a strength to the LBM.

There exist a convention for naming different lattices. A lattice of dimension d and with q distinct velocities is denoted by DdQq. For example a lattice with 9 velocities in dimension 2 is denoted D2Q9. An example of two different lattices is presented in fig, 3.2. The D2Q9 lattice is also the one that will be used in this work, the velocities $\mathbf{c}_i$ is given by

$$\{\mathbf{c}_i\} = \left\{ \begin{bmatrix} 0 \\ 0 \end{bmatrix}, \begin{bmatrix} 1 \\ 0 \end{bmatrix}, \begin{bmatrix} 0 \\ 1 \end{bmatrix}, \begin{bmatrix} -1 \\ 0 \end{bmatrix}, \begin{bmatrix} 0 \\ -1 \end{bmatrix}, \begin{bmatrix} 1 \\ 1 \end{bmatrix}, \begin{bmatrix} -1 \\ 1 \end{bmatrix}, \begin{bmatrix} -1 \\ -1 \end{bmatrix}, \begin{bmatrix} 1 \\ -1 \end{bmatrix} \right\} \tag{3.10}$$

To be able to retrieve the desired equations in the macroscopic limit of the LBE, the lattice used must possess a certain degree of isotropy. Thus the choice of lattice is not arbitrary. For instance, for obtaining the Navier-Stokes equations, the lattice must at least posses the following properties:

$$\sum_i w_i = 1 \tag{3.11}$$

16

$$\sum_i w_i c_{i\alpha} = 0 \tag{3.12}$$

$$\sum_i w_i c_{i\alpha} c_{i\beta} = c_s^2 \delta_{\alpha\beta} \tag{3.13}$$

$$\sum_i w_i c_{i\alpha} c_{i\beta} c_{i\gamma} = 0 \tag{3.14}$$

where the sums are over the discrete velocities $\mathbf{c}_i$, w_i are lattice specific weights c_s is the sound of speed for the lattice and δ_k is Kroenecker's delta.

The weights are introduced to compensate for the fact that different velocity vectors $\mathbf{c}_i$ is of different length. See for example the D2Q9 lattice in fig. 3.2b where three lengths are present. In this case, three different weights will be needed. From the relations in eqs. (3.11)(3.14) follow that these weights are:

$$w_i = \begin{cases} 4/9 & \text{if } i = 0 \\ 1/9 & \text{if } i = 1, 2, 3, 4 \\ 1/36 & \text{if } i = 5, 6, 7, 8 \end{cases} \tag{3.15}$$

The quantity c_s which often is referred to as the speed of sound is determined to

$$c_s = c/3 \tag{3.16}$$

where $c = |\mathbf{c}_{1,2,3,4}| = \delta_x/\delta_t$.

3.6 Asymptotic analysis

Methods from asymptotic analysis will, in this section, be used to investigate the macroscopic limit of the general LBE. More detailed and specific analyses for the three different equations considered will be presented in sections 3.7.1, 3.8.1 and 3.9.1.

Asymptotic analysis is basically about describing mathematical objects in some limit, e.g. how a function behaves for large or small values of some parameter. Consider for example the series S_ϵ:

$$S_\epsilon = a^{(0)} + a^{(1)}\epsilon + a^{(2)}\epsilon^2 + a^{(3)}\epsilon^3 + \mathcal{O}(\epsilon^4) \tag{3.17}$$

It is clear that for sufficiently small values of ϵ, the terms of higher order is negligible to those of lower order and the series may be truncated at some point and still be a good approximation of S_ϵ. For example if ϵ is small, then is $S_\epsilon \approx a^{(0)}$ and we say that if $a^{(1)} \neq 0$ that this approximation is of first order accuracy.

There are different approaches to go from the discrete LBE to a continuous macroscopic equation. The most frequently applied one to obtain the Navier-Stokes equations is the Chapman-Enskog method [7], which will reproduce the compressible equations.

An other method, often employed by M. Junk and his associates e.g. in [5], is a method based on regular asymptotic expansions, this is also the method that will be utilised in this work and will in the case of Navier-Stokes reproduce the incompressible equations. A brief discussion of the differences between the Chapman-Enskog and the regular expansion approaches will be carried out at the end of this chapter.

The basic idea behind the analysis is to expand the distribution function f_i in some small parameter, ϵ. Also this parameter will be related to the spatial and time scales. The macroscopic limit is obtained by taking the Taylor expansion of the discrete LBE and comparing terms of equal order in ϵ. Together with the fact that certain quantities is invariant under collisions, macroscopic differential equations is obtained. Now follows the part of the analysis which is common for the three equations, the more equation specific analysis is carried out in sections 3.7.1, 3.8.1 and 3.9.1 respectively.

3.6.1 Motivation of the choice of expansion parameter

A most desired property of the expansion parameter is that it should be a small and dimensionless number. If the lattice is dense enough with respect to the characteristic length scale of the system, a suitable choice is the Knudsen number, ϵ, which is defined as the ratio of the mean free path, δ_x, and the characteristic length of the system under consideration, ℓ_0, i.e. $\epsilon = \delta_x/\ell_o$. To be able to perform the asymptotic analysis we must also relate the time scale to this parameter. From the fact that the lattice speed $c_s = \delta_x/\delta_t$ and by introducing a characteristic speed, $u_o = \ell_0/t_0$, we have

$$\epsilon = \frac{\delta_x}{\ell_0} = \frac{c_s}{u_0}\frac{\delta_t}{t_0} \tag{3.18}$$

It is now clear that what determines the relation between the timescale and the parameter ϵ is the ratio of the characteristic speed and the lattice speed which is usually referred to as the Mach number, Ma. In our particular case we will operate in the incompressible limit, i.e. Ma $\ll 1$ and a suitable choice is a small number, thus Ma $= \epsilon$ is chosen [7]. The discretisation of the space and time step is then related through

$$\delta_x'^2 = \delta_t' = \epsilon^2 \tag{3.19}$$

where the primes denote dimensionless variables. This particular scaling is usually referred to as diffusive scaling.

3.6.2 Expanding the LBE

The LBE, eq. (3.5), with dimensionless variables and the BGK collision operator reads:

$$f_i(\mathbf{x}' + \epsilon\mathbf{c}_i', t' + \epsilon^2) - f_i(\mathbf{x}', t') = -\omega\left[f_i(\mathbf{x}', t') - f_i^{(eq)}(\mathbf{x}', t')\right]. \tag{3.20}$$

The primes denoting dimensionless variables will, for readability reasons, from hereon be dropped. If nothing else is stated we always consider dimensionless variables.

To obtain a differential equation, the difference equation in eq. (3.20) is Taylor expanded, which gives

$$\epsilon(\mathbf{c}_i \cdot \nabla f_i) + \epsilon^2(\partial_t f_i + (\mathbf{c}_i \cdot \nabla f_i)^2/2) + \epsilon^3(\partial_t(\mathbf{c}_i \cdot \nabla f_i) + (\mathbf{c}_i \cdot \nabla f_i)^3/6) + \mathcal{O}(\epsilon^4) = -\omega \left[f_i - f_i^{(eq)} \right]$$
(3.21)

Expanding also f_i and $f_i^{(eq)}$ in the parameter ϵ:

$$f_i = f_i^{(0)} + \epsilon f_i^{(1)} + \epsilon^2 f_i^{(2)} + \epsilon^3 f_i^{(3)} + \mathcal{O}(\epsilon^4)$$
(3.22)

$$f_i^{(eq)} = f_i^{(eq,0)} + \epsilon f_i^{(eq,1)} + \epsilon^2 f_i^{(eq,2)} + \epsilon^3 f_i^{(eq,3)} + \mathcal{O}(\epsilon^4)$$
(3.23)

and inserting these expressions into eq. (3.21) gives an equation with terms of varying orders of ϵ. Separating this equation in equations of common orders allows for an analysis of what happens at different scales of ϵ. For the four leading orders in ϵ we have:

$$\epsilon^0 : \quad 0 = -\omega \left[f_i^{(0)} - f_i^{(eq,0)} \right],$$
(3.24)

$$\epsilon^1 : \quad \mathbf{c}_i \cdot \nabla f_i^{(0)} = -\omega \left[f_i^{(1)} - f_i^{(eq,1)} \right],$$
(3.25)

$$\epsilon^2 : \quad \mathbf{c}_i \cdot \nabla f_i^{(1)} + \partial_t f_i^{(0)} + (\mathbf{c}_i \cdot \nabla f_i^{(0)})^2/2 = -\omega \left[f_i^{(2)} - f_i^{(eq,2)} \right]$$
(3.26)

and

$$\epsilon^3 : \quad \mathbf{c}_i \cdot \nabla f_i^{(2)} + \partial_t f_i^{(1)} + (\mathbf{c}_i \cdot \nabla f_i^{(1)})^2/2 + \partial_t(\mathbf{c}_i \cdot \nabla f_i^{(0)}) + (\mathbf{c}_i \cdot \nabla f_i^{(0)})^3/6 = -\omega \left[f_i^{(3)} - f_i^{(eq,3)} \right].$$
(3.27)

The idea is now that for an equation of a particular order in ϵ, use collision invariants and eliminate unknown $f_i^{(n)}$:s by using equations of lower order in ϵ. This will in the end result in differential equations for macroscopic variables, given by moments of the f_i:s.

3.7 LBM for the Nernst-Planck equation

The method presented here is based on representing the Nernst-Planck equation, eq. (2.8), as an equation of advection-diffusion type. Considering the quantity:

$$\bar{\mathbf{u}} = \mathbf{u} - \frac{z q_e D}{k_B T} \nabla \psi$$
(3.28)

as an effective advective velocity, we have:

$$\frac{\partial \rho}{\partial t} + \nabla \cdot (\bar{\mathbf{u}} \rho - D \nabla \rho) = 0$$
(3.29)

19

which is a mass conservation equation with fluxes from diffusion and from advection respectively. The letter c for denoting the charge concentration has in this section been replaced by the letter ρ for avoiding the risk of confusing it with the lattice velocities which traditionally are denoted by $\mathbf{c}_i$.

A collision operator of BGK type, eq. (3.8) will be used together with a D2Q9 lattice. The lattice-Boltzmann equation then reads:

$$f_i(\mathbf{x} + \mathbf{c}_i \delta_t, t + \delta_t) - f_i(\mathbf{x}, t) = -\omega \left[f_i(\mathbf{x}, t) - f_i^{(eq)}(\mathbf{x}, t) \right] \tag{3.30}$$

with $\{\mathbf{c}_i\}_{i=0}^{Q-1}$ for the D2Q9 lattice as in eq. (3.10). The equilibrium function, $f_i^{(eq)}$, is chosen as [8]:

$$f_i^{(eq)} = w_i \rho \left(1 + \frac{\mathbf{c}_i \cdot \bar{\mathbf{u}}}{c_s^2} \right) \tag{3.31}$$

with the weights, w_i, as in eq. (3.15). The charge density and charge flux density is obtained by taking the zeroth and first moments of the distribution function respectively, i.e:

$$\rho = \sum_i f_i \tag{3.32}$$

and

$$\mathbf{j} = \sum_i f_i \mathbf{c}_i \tag{3.33}$$

The diffusion constant, D, is related to the relaxation parameter ω through

$$D = c_s^2 \left(\frac{1}{2} - \frac{1}{\omega} \right). \tag{3.34}$$

3.7.1 Asymptotic analysis

To motivate the appearance of the above suggested method for solving eq. (3.29) and for showing under what premises the method is valid, the macroscopic limit of the discrete scheme will now be analysed in an asymptotic manner. Note that for the advection diffusion equation mass will be conserved but flux will not be conserved.

From the expansion of f_i in eq. (3.22) and from eqs. (3.49) and (3.50) follow the expansions of the mass density and flux respectively as

$$\rho = \rho^{(0)} + \epsilon \rho^{(1)} + \epsilon^2 \rho^{(2)} + \epsilon^3 \rho^{(3)} + \mathcal{O}(\epsilon^4) \tag{3.35}$$

and

$$\mathbf{j} = \mathbf{j}^{(0)} + \epsilon \mathbf{j}^{(1)} + \epsilon^2 \mathbf{j}^{(2)} + \epsilon^3 \mathbf{j}^{(3)} + \mathcal{O}(\epsilon^4) \tag{3.36}$$

The advective velocity is also expanded as:

$$\bar{\mathbf{u}} = \bar{\mathbf{u}}^{(0)} + \epsilon\bar{\mathbf{u}}^{(1)} + \epsilon^2\bar{\mathbf{u}}^{(2)} + \epsilon^3\bar{\mathbf{u}}^{(3)} + \mathcal{O}(\epsilon^4) \tag{3.37}$$

By plugging these expansion into the equilibrium distribution eq. (3.31), the expansion in eq. (3.23) is obtained. The terms of order zero is used in the zeroth order equation of the LBE, eq. (3.24), which gives

$$f_i^{(0)} = w_i\rho^{(0)}\left(1 + \frac{\mathbf{c}_i \cdot \bar{\mathbf{u}}^{(0)}}{c_s^2}\right). \tag{3.38}$$

However, since we are only considering advection in the low Mach limit, i.e. $|\bar{\mathbf{u}}| \sim \epsilon$, we will in this analysis assume that $\bar{\mathbf{u}}^{(0)} = 0$. $\bar{\mathbf{u}}$ will then be of order ϵ to leading order. It is possible to show [5] that this assumption holds if $\bar{\mathbf{u}}$ is initialised properly, i.e. small and if no major momentum sources are present. Thus the expression for $f_i^{(0)}$ reduces to

$$f_i^{(0)} = w_i\rho^{(0)}. \tag{3.39}$$

We now continue to the equation of order one in ϵ, eq. (3.25). Taking the zeroth moment gives the equation $0 = 0$ which indeed is true but not very useful. Note that the right hand side vanishes due to mass conservation. $f_i^{(1)}$ will be needed in the next step and is, by using eq. (3.39):

$$f_i^{(1)} = -\frac{1}{\omega}(\mathbf{c}_i \cdot \nabla)(w_i\rho^{(0)}) + w_i\left(\rho^{(1)} + \rho^{(0)}\frac{\mathbf{c}_i \cdot \bar{\mathbf{u}}^{(1)}}{c_s^2}\right). \tag{3.40}$$

Taking the first moment of $f_i^{(1)}$ gives the leading order in the flux ($\mathbf{j}^{(0)} = 0$ since $\bar{\mathbf{u}}^{(0)} = 0$):

$$\mathbf{j}^{(1)} = \rho^{(0)}\bar{\mathbf{u}}^{(1)} - c_s^2/\omega\nabla\rho^{(0)} \tag{3.41}$$

Continuing to the equation of order two in ϵ, eq. (3.26) and taking the zeroth moment of the equation gives

$$\nabla \cdot \mathbf{j}^{(1)} + \partial_t\rho^{(0)} + c_s^2/2\nabla^2\rho^{(0)} = 0 \tag{3.42}$$

and by inserting the expression for $\mathbf{j}^{(1)}$ we end up with

$$\partial_t\rho^{(0)} + \nabla \cdot \left[\rho^{(0)}\bar{\mathbf{u}}^{(1)} - c_s^2\left(\frac{1}{\omega} - \frac{1}{2}\right)\nabla\rho^{(0)}\right] = 0 \tag{3.43}$$

which is an advection diffusion equation with a diffusion constant as in eq. (3.34). Since $\rho^{(0)}$ fulfils the equation of interest, the solution ρ that we get from the lattice-Boltzmann method is at least of first order accuracy. To determine the exact order of accuracy, higher order terms, $\rho^{(k>0)}$, must be determined. If also all those terms would be zero the method would be exact, unfortunately that is not the case. The analysis of higher order terms will not be performed here, but it is possible to show that $\rho^{(1)}$ is zero only under certain premises, i.e. for a proper initialisation [8]. $\rho^{(2)}$ is however in general non-zero and the obtained solution is thus second order accurate.

3.8   LBM for the incompressible Navier-Stokes

The most frequent use of the LBM is to solve the Navier-Stokes equations. In this work only the incompressible case, eqs. (2.22) and (2.23) will be considered. The LBM may however be used to reproduce weak compressibility [4]. The incorporation of forces will be treated in section 3.8.2. We recall the incompressible Navier-Stokes equations without external forces present from chapter 2 as:

$$\nabla \cdot \mathbf{u} = 0 \tag{3.44}$$

and

$$\rho \left(\frac{\partial \mathbf{u}}{\partial t} + \mathbf{u} \cdot \nabla \mathbf{u} \right) = -\nabla P + \rho \nu \nabla^2 \mathbf{u} \tag{3.45}$$

where ν is the kinematic viscosity related through the dynamic viscosity, μ, by

$$\mu = \rho \nu. \tag{3.46}$$

A LBM will now be formulated for eqs. (3.44) and (3.45). The LBE with a BGK collision operator is given by

$$f_i(\mathbf{x} + \mathbf{c}_i \delta_t, t + \delta_t) - f_i(\mathbf{x}, t) = -\omega \left[f_i(\mathbf{x}, t) - f_i^{(eq)}(\mathbf{x}, t) \right] \tag{3.47}$$

where

$$f_i^{(eq)} = w_i \rho \left[1 + \frac{\mathbf{c}_i \cdot \mathbf{u}}{c_s^2} + \frac{(\mathbf{c}_i \cdot \mathbf{u})^2}{2c_s^4} - \frac{\mathbf{u}^2}{2c_s^2} \right] \tag{3.48}$$

where w_i are the weights in eq. (3.15).

The density, ρ, and the mass flux, $\rho\mathbf{u}$, is determined from f_i by taking the zeroth and first moments respectively:

$$\rho = \sum_i f_i \tag{3.49}$$

and

$$\rho\mathbf{u} = \sum_i f_i \mathbf{c}_i. \tag{3.50}$$

The kinematic viscosity is related to the relaxation parameter, ω

$$\nu = c_s^2 \left(\frac{1}{\omega} - \frac{1}{2} \right). \tag{3.51}$$

3.8.1 Asymptotic analysis

Partially based on [5], an asymptotic analysis of the above suggested method will be performed. In most literature available, when reproducing the Navier-Stokes equations in the macroscopic limit, a Chapman-Enskog expansion is performed. Note that this is *not* what is used here.

From the expansion of f_i in eq. (3.22) follows the expansion of the macroscopic mass and velocity as

$$\rho = \rho^{(0)} + \epsilon\rho^{(1)} + \epsilon^2\rho^{(2)} + \epsilon^3\rho^{(3)} + \mathcal{O}(\epsilon^4) \tag{3.52}$$

and

$$\mathbf{u} = \mathbf{u}^{(0)} + \epsilon\mathbf{u}^{(1)} + \epsilon^2\mathbf{u}^{(2)} + \epsilon^3\mathbf{u}^{(3)} + \mathcal{O}(\epsilon^4). \tag{3.53}$$

These expansions are plugged into the equilibrium distribution in eq. (3.48) and from the equation of order zero in ϵ, eq. (3.24)section gives:

$$f_i^{(0)} = w_i\rho^{(0)} \tag{3.54}$$

Here $\mathbf{u}^{(0)}$ has been assumed to be zero by the same argumentation as in the Nernst-Planck analysis, section 3.7.1. Continuing to the equation of order 1 in ϵ, eq. (3.25) and taking the first moment gives

$$\nabla\rho^{(0)} = 0 \tag{3.55}$$

3.8.2 Forcing schemes

how to add a "forcing" term in the method.

3.9 LBM for Poisson's equation

As Poisson's equation, eq. (2.1) is considered, a fundamental difference to the Nernst-Planck and Navier-Stokes equations is imediatley noted. It is not a differential equation of parabolic but of elliptic type. If we consider what has been said about the LBM so far in this chapter, it seems that it is a method that deals with parabolic equations and not elliptic. However, by introducing a time derivative to the Poisson's equation and only considering the steady state solution the LBM may be used even for this equation. A diffusion-like equation with a source term is then obtained

$$\partial_t\rho + \nabla^2\rho = \mathrm{R} \tag{3.56}$$

where R is the right-hand side of the Poisson's equation.

A LBM for this equation will now be formulated. The LBE to be solved in this case is, an equation of the form:

$$f_i(\mathbf{x} + \mathbf{c}_i\delta_t, t + \delta_t) - f_i(\mathbf{x}, t) = -\omega \left[f_i(\mathbf{x}, t) - f_i^{(eq)}(\mathbf{x}, t) \right] + G_i(R) \tag{3.57}$$

where $G_i(R)$ is an addition to the BGK collision operator to account for the source term R in eq. (3.56). The equilibrium distribution is given by

$$f_i^{(eq)} = w_i\rho \tag{3.58}$$

where w_i are the weights in eq. (3.15).

The quantity ρ which in this work is interpreted to electric potential in the steady state is determined by

$$\rho = \sum_i f_i \tag{3.59}$$

and the quantity which, to us, is of even more interest, i.e. the electric field, is given by

$$\nabla\rho = -\frac{\omega}{c_s^2\delta_x} \sum_i f_i\mathbf{c}_i. \tag{3.60}$$

Finally, the addtional source term in the collision operator, $G_i(R)$, is given by

$$G_i(R) = w_ic_s^2\left(\frac{1}{2} - \frac{1}{\omega}\right)R. \tag{3.61}$$

3.9.1 Asymptotic analysis

The given method for solving eq. (3.56) will now be motivated by preforming an asymptotic analysis of the suggested LBE.

f_i is expanded as in eq. (3.22) which gives an exansion of ρ as in eq. (3.35). Further is the source term R expanded into

$$R = R^{(0)} + \epsilon R^{(1)} + \epsilon^2 R^{(2)} + \epsilon^3 R^{(3)} + \mathcal{O}(\epsilon^4) \tag{3.62}$$

which also gives an expansion for the LBE source term as

$$G_i = G_i^{(0)} + \epsilon G_i^{(1)} + \epsilon^2 G_i^{(2)} + \epsilon^3 G_i^{(3)} + \mathcal{O}(\epsilon^4). \tag{3.63}$$

The equilibrium distribution is expanded by plugging in the expansion of ρ from eq. (3.35). This gives for the zeroth order equation in ϵ, eq. (3.24) that

$$f_i^{(0)} = w_i\rho^{(0)} + \frac{1}{\omega}G_i^{(0)} \tag{3.64}$$

However, taking the first moment of the equation gives $G_i^{(0)} = 0$ and the above expression for $f_i^{(0)}$ reduces to

$$f_i^{(0)} = w_i\rho^{(0)}. \tag{3.65}$$

Coninuing to the equation of first order in ϵ, eq. (3.25) and taking the zeroth moment gives that also $G_i^{(1)} = 0$. Taking the first moment of the same equation gives

$$\nabla \rho^{(0)} = -\frac{\omega}{c_s^2} \sum_i f_i^{(1)} \mathbf{c}_i \approx -\frac{\omega}{c_s^2 \delta_x} \sum_i f_i \mathbf{c}_i \tag{3.66}$$

Here, for the approximation, the expansion of f_i is used together with the fact that $\epsilon = \delta_x$ in dimensionless variables.

The next equation in ϵ, i.e. the one of order two, will eventually give us what we are looking for. Taking the zeroth moment gives

$$-\frac{c_s^2}{\omega}\nabla^2\rho^{(0)} + \partial_t\rho^{(0)} + \frac{c_s^2}{2}\nabla^2\rho^{(0)} = \sum_i G_i^{(2)}(R^{(2)}) \tag{3.67}$$

From this equation, it is deduced that in order to obtain Poisson's equation in a steady state situation, i.e. when $\partial_t\rho^{(0)} = 0$ the right-hand side must fulfill the follwong condition

$$\sum_i G_i^{(2)}(R^{(2)}) = c_s^2 \left(\frac{1}{2} - \frac{1}{\omega}\right) R^{(2)} \tag{3.68}$$

One such $G_i^{(2)}(R)$ is the one described in eq. (3.61).

3.10 Algorithm/Scheme for solving the coupled equations

the iterative scheme used.

3.11 Boundary conditions

discussion and description of the boundary conditions

3.11.1 bounce back

accuracy, e.g. second order accurate if placed between node planes...

3.11.2 slip

3.11.3 he-zou, constant density/velocity

3.11.4 Maybe something on non-local boundary conditions

3.12 Physical units vs lattice units

how to interchange between them... etc...

3.13 Chapman-Enskog vs regular expansion analysis

4

A few notes on high performance computing

intro what is said below refer to computers of a certain architecture...

4.1   The pipeline

keep it full.

4.2   Locality

using the caches in a good way. some examples of its importance.

4.2.1   Locality and LBM

4.3   Parallelisation

shared memory, distributed memory...
    data dependence, LBM good!
    OpenMP/MPI

4.4   Maybe something about profiling

men kanske inte tillför något vettigt.

4.5 Choice of programming language

4.6 Some stats on the performance of the code...

Lattice updates/s

5

Model benchmarks

intro 2D

5.1 Poiseuille flow

First out for evaluating the LBM solver of the Navier-Stokes equations is the situation with Poiseuille flow. This is a classic example and one of the easiest situations were the NS equations are exact solvable. Consider a 2D channel of length l and width H. If the flow in this channel is driven by a constant force, e.g. a constant pressure drop, the velocity profile will adopt to a parabolic shape in the steady state situation. Here follows a brief derivation of the exact expression for the velocity profile.

Consider the (non-dimensional) Navier-Stokes eqs. (??) and (??) in 2D. Let x be the direction along the channel and y the direction across the channel. In the case of a pressure gradient in the x direction and no other external forces involved we deduce that the y component of the velocity is zero. Thus eq. (??) reduces to an equation for the x component of the velocity

$$\frac{\partial u_x}{\partial t} - u_x \frac{\partial u_x}{\partial x} = \frac{1}{Re} \frac{\partial^2 u_x}{\partial y^2} - \frac{\partial P}{\partial x}. \tag{5.1}$$

Under the assumption of a system in a steady state, i.e. $\partial u_x / \partial t = 0$. Further if the flow is fully developed $\partial u_x / \partial x = 0$, this also assures that (??) is fulfilled. We now have together with writing the constant pressure gradient as $\Delta P / l$

$$\frac{\partial^2 u_x}{\partial y^2} = \frac{Re\ \Delta P}{l}. \tag{5.2}$$

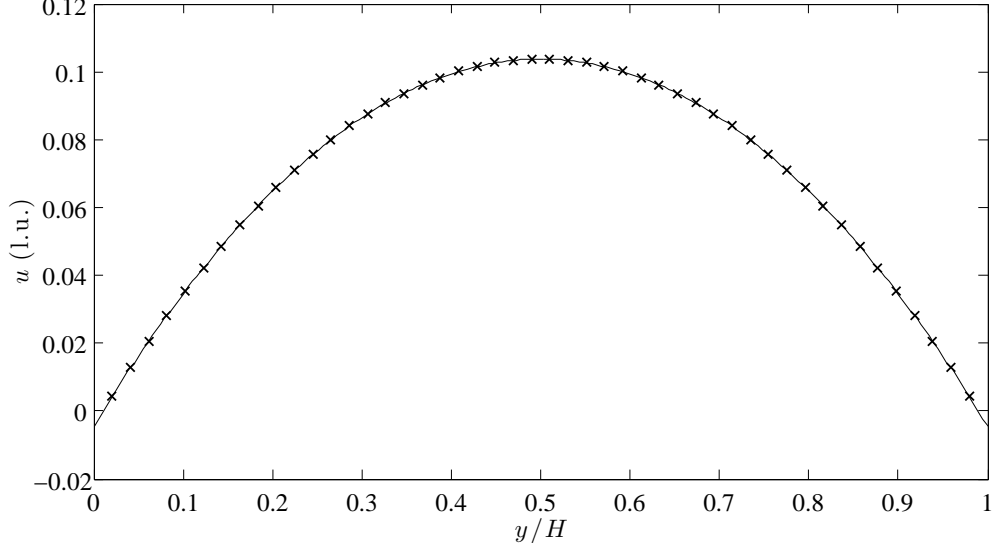Solving this eq. with no slip boundary conditions, $u_x(0) = u_x(H) = 0$ gives an expression of the velocity profile

Figure 5.1: Obtained velocity profiles of Poiseuille flow ($\times$) compared to the analytical solution (solid line). A grid of 3×50 nodes were used. There was also no variation of the velocity field in the flow direction (not shown in this figure). The velocity is given in lattice units.

$$u_{x}(y) = \frac{\mathrm{Re}\,\Delta\mathrm{P}}{2l}y(y - H).\tag{5.3}$$

The benchmark of the LBM solver of the NS equation described in section 3.8 was performed with a pressure gradient incorporated as a force. Other possibilities would be to drive the fluid by imposing fixed pressures/velocities at the inlet and outlet. In this case, with a driving force, periodic boundary conditions were imposed at the inlet and outlet. At the channel walls, the bounce-back boundary condition described in section **??** was imposed. The actual boundary will thus be located half a node-node distance into the fluid.

A grid with 50 nodes across the channel and 3 in the flow direction were used. The driving force was set to $\Delta\mathrm{P}/l = 1\cdot10^{-4}$ and the Reynolds number to $\mathrm{Re} = l_0 u_0/\nu$ where the viscosity is $\nu = 0.2778$ from eq. (**??**) with $\omega = 0.75$ and $l_0 = u_0 = 1$. The solution that was obtained after 20000 iterations is presented in fig. 5.1. The analytical solution, eq. (5.3), is plotted for comparison.

The agreement between computed and analytical solution is satisfying. With an RMS error of $9.271\cdot10^{-5}$ l.u. and maximum absolute error of $1.198\cdot10^{-4}$ l.u.. Note that the actual boundary is located half a node-node distance into the computational domain, this is due to the implementation of the bounce-back scheme, see section **??**.

5.2 Taylor-Green vortex

5.3 Helmholtz equation

The LB formulation for solving Poisson's equation as well as the implementation was tested by solving Helmholtz equation with a certain set of boundary conditions allowing for finding an analytical solution. The homogeneous Helmholtz equation reads:

$$\nabla \psi = \lambda^2 \psi \tag{5.4}$$

where λ is a real parameter. The equation was solved for $\lambda = 2$ on the domain $(x, y) \in [0, 1] \times [0, 1]$ with the following Dirichlet boundary conditions:

$$\psi(0, y) = -\psi(1, y) = \frac{\sinh \sqrt{\lambda^2 + \pi^2}(1-y)}{\sinh \sqrt{\lambda^2 + \pi^2}},$$
$$\psi(x, 0) = \cos \pi x, \ \ \psi(x, 1) = 0. \tag{5.5}$$

The analytical solution to eq. (5.4) with the given boundary conditions is [9]:

$$\psi(x, y) = cos\pi x \frac{\sinh \sqrt{\lambda^2 + \pi^2}(1 - y)}{\sinh \sqrt{\lambda^2 + \pi^2}}. \tag{5.6}$$

A grid of $n_x \times n_y = 65 \times 65$ nodes was used when computing the LBM solution. The computational domain was rescaled to the desired one by setting $\delta_x = 1/(n_x - 1) = 1/64$ and $\delta_t = \delta_x^2$. An other possibility would have been to rescale the parameter λ and have $\delta_x = \delta_t = 1$.

The boundary conditions in eq. (**??**) was implemented using the He/Zou approach described in section **??**. A bounce back approach with some momentum addition would also have been possible but was not chosen due to that the actual boundary location is not at the node location, but half a node-node distance into the computational domain. Also the bounce-back implementation is previously tested.

In fig. 5.2a, the obtained solution is presented together with the absolute error in fig. 5.2b. The agreement is satisfying, with an error which magnitude is about the same as in previous works [9]. The error takes on its maximum at the boundary of the domain, implying that the fulfilment of the boundary conditions is not complete.

5.4 Advection-Diffusion

Before the implementation of the Nernst-Planck part of the model is tested, a special case is considered, i.e. when the electrical potential in the domain is constant. This makes the flux term including the electrical potential in eq. (2.8) vanish and we have to solve only for pure advection and diffusion.

Introducing characteristic scales for the concentration (c_0), advective velocity (u_0) and length (l_0) respectively, gives the non-dimensional advection-diffusion equation:

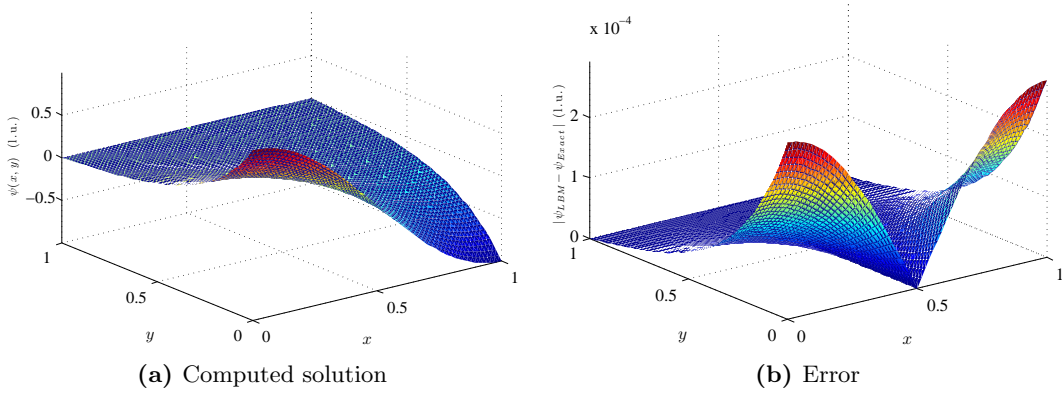**(a)** Computed solution

(b) Error

Figure 5.2: To the left, the obtained solution of the Helmholtz equation, eq. (5.4). To the right, the error.

$$\frac{\partial c}{\partial t} + \mathbf{u} \cdot \nabla c - \frac{D}{u_0 l_0} \nabla^2 c = 0. \tag{5.7}$$

All variables in (5.7) are non-dimensional. The quantity $\text{Pe} = u_0 l_0/D$ is often referred to as the Péclet number. It determines the relation between contributions to the dynamics from advection and diffusion respectively. For $\text{Pe} \gg 1$ the dynamics is dominated by advection and for $\text{Pe} \ll 1$ by diffusion.

The LB model described in section 3.7 was tested by studying the evolution in time and space of a point mass in one dimension. The analytical solution of eq. (5.7) in one dimension with initial conditions $c(x, t = 0) = \delta(x)$ on an infinite domain is:

$$c(x,t) = \sqrt{\frac{\text{Pe}}{4\pi t}} \exp\left(-\frac{(x-ut)^2 \text{Pe}}{4t}\right). \tag{5.8}$$

In the numerical computations the parameters $\text{Pe} = 10$ and $|\mathbf{u}| = 0.1$ were used. The domain consisted of 200 lattice nodes and three snapshots in time at $t = 100, 200, 300$ l.u. were compared to the analytical solution. The result is presented in fig. 5.3.
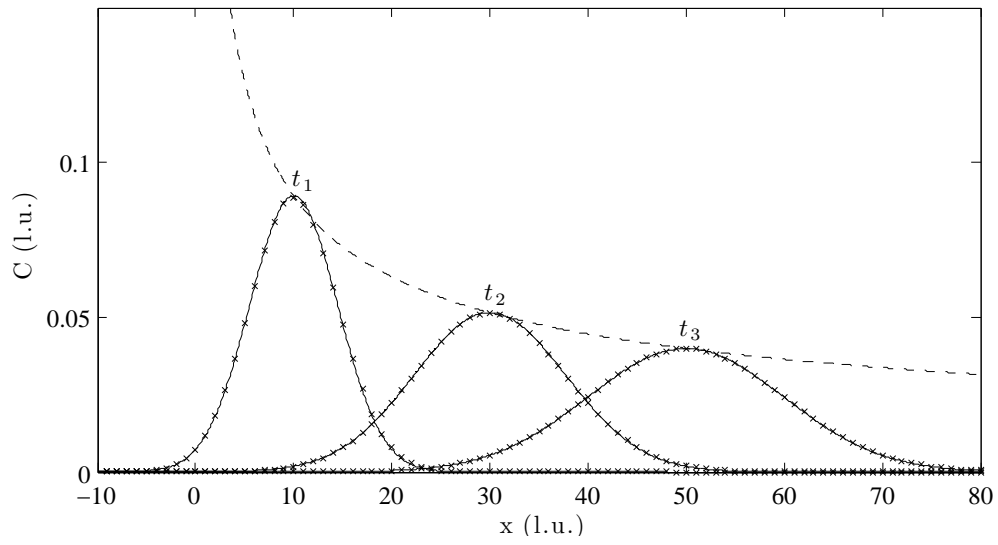
5.5 Nernst-Planck, a special case

Figure 5.3: Obtained solutions ($\times$) of the advection-diffusion equation for a point mass evolving in time and space. Three different times ($t_n = 100n$) are compared to analytical solutions (solid). The Amplitude of the solutions as function of time has also been plotted (dashed). The advecting velocity, $u_0 = 0.1$ was used together with a Peclet number, Pe $= 10$. All units are in lattice units.

6

Modelling of electrokinetic flow

6.1 Electric potential in 2D channel - PB

section in the channel, + debye-huckel comparision

6.1.1 It might be interesting to compare the two models Chai and Wang

6.2 Compare with Nernst-Planck

6.2.1 Potential

6.2.2 Charge distribution

6.3 Electroviscous effect

NP + PB differences?

6.4 Flow in array of charged squares

maybe other geometries as well?

6.5 3D?

only god knows...

7

Conclusions

And what do we conclude of this?

Bibliography

[1] D. Li, Electrokinetics In Microfluidics, Interface Science and Technology Series, Academic Press, 2004.
URL `http://books.google.se/books?id=1QkpluJqQegC`

[2] D. Hlushkou, D. Kandhai, U. Tallarek, Coupled lattice-boltzmann and finite-difference simulation of electroosmosis in microfluidic channels, International Journal for Numerical Methods in Fluids 46 (5) (2004) 507–532.
URL `http://dx.doi.org/10.1002/fld.765`

[3] S. Succi, M. Sbragaglia, S. Ubertini, Lattice boltzmann method, Scholarpedia 5 (5) (2010) 9507.

[4] D. Wolf-Gladrow, Lattice-Gas Cellular Automata and Lattice Boltzmann Models: An Introduction, no. v. 1725 in Lecture Notes in Mathematics, Springer, 2000.
URL `http://books.google.se/books?id=cHcpWgxAUu8C`

[5] M. Junk, A. Klar, L.-S. Luo, Asymptotic analysis of the lattice boltzmann equation, Journal of Computational Physics 210 (2) (2005) 676 – 704.
URL `http://www.sciencedirect.com/science/article/pii/S0021999105002573`

[6] Wolfram Alpha, Information content of the web - wolfram alpha (November 2012).
URL `http://www.wolframalpha.com/input/?i=estimated+data+content+of+the+web`

[7] M. Junk, Z. Yang, Assymptotic Analysis of Lattice Boltzmann Boundary Conditions, Journal of Statistical Physics 121 (2005) 3–35.

[8] Alexey's och Tobias' artikel.., , ??Article in press...

[9] Z. Chai, B. Shi, A novel lattice Boltzmann model for the Poisson equation, Applied Mathematical modeling 32 (2007) 2050–2058.